Weak η^2-Olefin Bonding in Palladium and Platinum Allyl Cationic Complexes Containing Chiral Monodentate Ligands with α-Phenyl Methyl Amine Side Chains

Serena Filipuzzi, Paul S. Pregosin,* Maria José Calhorda,* and Paulo J. Costa

Laboratory of Inorganic Chemistry, ETH HCI, Hönggerberg CH-8093 Zürich, Switzerland, Departamento de Química e Bioquímica, CQB, Faculdade de Ciências, Universidade de Lisboa, Campo Grande, 1749-016 Lisboa, Portugal, and Departamento de Química, CICECO, Universidade de Aveiro, 3810-193, Aveiro, Portugal

Detailed NMR studies on a series of Pd and Pt allyl complexes containing phosphoramidite ligands with NCH(CH₃)Ph side chains are reported. When a coordination position becomes available, e.g., via abstraction of a chloride ligand, one double bond of the phenyl group of the side chain complexes to the metal, affording an η^2-olefin structure. These allyl complexes exhibit a number of dynamic processes, and these have been elucidated via low-temperature NMR studies combined with 2D NOESY methods. DFT calculations confirm the ability of the amine side chain to coordinate to the metal almost without distortion, leading to a weak η^2-arene−Pd bonding interaction (~13 kcal mol^{-1}). The latter result is supported by the NMR studies.

Introduction

There is an increasing interest in chiral monodentate P-donors,[1,2] as these have been found to be valuable in a variety of organic transformations.[1–4] Occasionally, one finds reports suggesting that these ligands (and related bidentate phosphine donors) are capable of coordinating a somewhat remote double bond from the organic backbone. This is certainly the case for the monodentate biaryl-based MOP[5,6] and bidentate Binap[7,8]
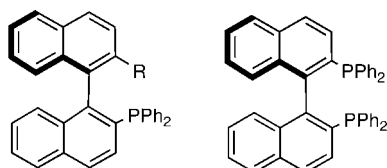

MOP (with differing R substituents)   Binap

ligands. For MOP, the double bond adjacent to the R-group and, for Binap, the double bond adjacent to the PPh₂ moiety

have both been found to be capable of complexing a transition metal. A number of related complexation modes have also been reported.[9]

An increasing number of papers concern themselves with the use of phosphoramidite ligands, e.g., **1**, in various homogeneously catalyzed reactions.[10,11] Ligand **1** possesses three
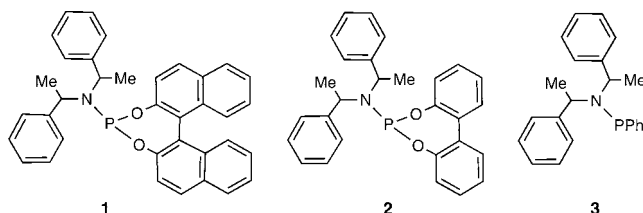
1   **2**   **3**

stereogenic fragments, and a wide variety of differently substituted phosphoramidite derivatives are now in use. Interestingly, it has been recently reported[12,13] that the π-system of one of the amino-aryl fragments of **1** can interact with a Ru(II) center, as indicated below, and thus stabilize an otherwise reactive 16*e* species.

---

* Corresponding author. E-mail: pregosin@inorg.chem.ethz.ch.

(1) Ansell, J.; Wills, M. *Chem. Soc. Rev.* **2002**, *31* (5), 259–268.

(2) Jerphagnon, T.; Renaud, J.-L.; Bruneau, C. *Tetrahedron: Asymmetry* **2004**, *15*, 2101–2111.

(3) (a) Polet, D.; Alexakis, A.; Tissot-Croset, K.; Corminboeuf, C.; Ditrich, K. *Chem.−Eur. J.* **2006**, *12* (13), 3596–3609. (b) Boele, M. D. K.; Kamer, P. C. J.; Lutz, M.; Spek, A. L.; de Vries, J. G.; van Leeuwen, P.; van Strijdonck, G. P. E. *Chem.−Eur. J.* **2004**, *10* (24), 6232–6246. (c) Hayashi, T. *J. Organomet. Chem.* **1999**, *576* (1−2), 195–202. (d) Helmchen, G.; Dahnz, A.; Duebon, P.; Schelwies, M.; Weihofen, R. *Chem. Commun.* **2007**, (7), 675–691.

(4) Feringa, B. L. *Acc. Chem. Res.* **2000**, *33*, 346–353.

(5) Kumar, P. G. A.; Dotta, P.; Hermatschweiler, R.; Pregosin, P. S.; Albinati, A.; Rizzato, S. *Organometallics* **2005**, *24* (6), 1306–1314.

(6) Dotta, P.; Kumar, P. G. A.; Pregosin, P. S.; Albinati, A.; Rizzato, S. *Organometallics* **2003**, *22* (25), 5345–5349.

(7) (a) Geldbach, T. J.; Pregosin, P. S. *Eur. J. Inorg. Chem.* **2002**, 1907–1918. (b) den Reijer, C. J.; Dotta, P.; Pregosin, P. S.; Albinati, A. *Can. J. Chem.* **2001**, *79*, 693–704. (c) Geldbach, T. J.; Pregosin, P. S.; Rizzato, S.; Albinati, A. *Inorg. Chim. Acta* **2006**, *359* (3), 962–969.

(8) Costa, P. J.; Calhorda, M. J.; Pregosin, P. S. *Collect. Czech. Chem. Commun.* **2007**, *72* (5−6), 703–714.

(9) (a) Faller, J. W.; Sarantopoulos, N. *Organometallics* **2004**, *23* (9), 2008–2014. (b) Kocovsky, P.; Vyskocil, S.; Cisarova, I.; Sejbal, J.; Tislerova, I.; Smrcina, M.; Lloyd-Jones, G. C.; Stephen, S. C.; Butts, C. P.; Murray, M.; Langer, V. *J. Am. Chem. Soc.* **1999**, *121* (33), 7714–7715. (c) Wang, Y.; Li, X.; Sun, J.; Ding, K. *Organometallics* **2003**, *22* (9), 1856–1862.

(10) (a) Welter, C.; Dahnz, A.; Brunner, B.; Streiff, S.; Dübon, P.; Helmchen, G. *Org. Lett.* **2005**, *7* (7), 1239–1242. (b) Tissot-Croset, K.; Polet, D.; Alexakis, A. *Angew. Chem., Int. Ed.* **2004**, *43* (18), 2426–2428. (c) Kiener, C. A.; Shu, C.; Incarvito, C.; Hartwig, J. F. *J. Am. Chem. Soc.* **2003**, *125* (47), 14272–14273. (d) Imbos, R.; Minnaard, A. J.; Feringa, B. L. *J. Chem. Soc., Dalton Trans.* **2003**, (10), 2017–2023.

(11) (a) Arnold, L. A.; Imbos, R.; Mandoli, A.; de Vries, A. H. M.; Naasz, R.; Feringa, B. L. *Tetrahedron* **2000**, *56*, 2865–2878. (b) Reetz, M. T.; Ma, J. A.; Goddard, R. *Angew. Chem., Int. Edit.* **2005**, *44*, 412–415.

(12) Huber, D.; Kumar, P. G. A.; Pregosin, P. S.; Mikhel, I. S.; Mezzetti, A. *Helv. Chim. Acta* **2006**, *89* (8), 1696–1715.

(13) Huber, D.; Kumar, P. G. A.; Pregosin, P. S.; Mezzetti, A. *Organometallics* **2005**, *24* (22), 5221–5223.

---

structure fragment from ref. 12,13
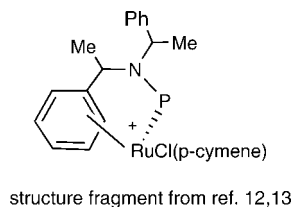
In order to further explore this possible bonding mode, as well as the dynamics that might accompany such an interaction, we have prepared a series of palladium(II) and, to a lesser extent, platinum(II) allyl complexes using ligands **1**−**3** and describe here their NMR characteristics. Compounds **2** and **3** are both interesting and relevant as they (a) have been successfully used as auxiliaries in enantioselective catalysis[14,15] and (b) reduce the complexity of the NMR analysis relative to that for **1**. DFT calculations confirm the ability of the amine side chain to coordinate the metal almost without distortion, leading to a weak η^2-arene−Pd bonding interaction (∼13 kcal mol^{-1}). The latter result is supported by the NMR studies.

Results and Discussion

The cationic allyl complexes were prepared[16] in a straightforward fashion, as indicated in Scheme 1, by first treating the appropriate metal(allyl)chloro-bridged dinuclear species with 2 equiv of the P-donor, to afford the mononuclear chloro compounds. Subsequent abstraction of the chloride ligand using AgSbF$_6$ affords the new cationic salts. Selected ^{13}C NMR data for the mononuclear chloro derivatives, **4**−**14**, are given in Table 1, while the pertinent ^{13}C NMR data for the various Pd and Pt allyl cationic complexes, **15**−**25**, are given in Tables 2 and 3. In most of the salts the NMR spectra showed two isomeric species, in almost equal quantities, due to the *exo* and *endo* orientations of the allyl with respect to the chelating ligand. Although we find about equal quantities of the two species, in the tables these are always identified as "major" and "minor". We find only modest differences in the NMR characteristics of these two isomers. Nevertheless, the presence of isomers results in a significant complication of the proton spectroscopy, with the result that a high-field instrument (700 MHz) was required in order to (a) assign all of the various protons and then (b) correlate these to their appropriate ^{13}C signals. Table 4 gives ^{31}P data for all of the cationic complexes, and an extensive list of ^{1}H chemical shifts can be found in the Supporting Information. Except for one Pt complex, **24**, the data were obtained at low temperature in order to slow the various intramolecular exchange processes.

The low-temperature NMR results are consistent with a structure such as **26** for all of the cations; that is, one double bond of the pendant phenyl ring, involving C1 and C2, is complexed. This conclusion arises primarily from the ^{13}C results of Table 3. In this compilation the chemical shifts of the carbons C1, C2, and C6 from the amine side chain are highlighted, and it is convenient to start with the three Pt salts, **23**−**25**. The changes in the chemical shifts, Δδ, are given with respect to chloro complexes, as these represent better models than the free

(14) Palais, L.; Mikhel, I. S.; Bournaud, C.; Micouin, L.; Falciola, C. A.; Vuagnoux-d'Augustin, M.; Rosset, S.; Bernardinelli, G.; Alexakis, A. *Angew. Chem., Int. Ed.* **2007**, *46* (39), 7462–7465.

(15) Alexakis, A.; Polet, D.; Benham, C.; Rosset, S. *Tetrahedron: Asymmetry* **2004**, *15* (14), 2199–2203.

(16) The compound [Pd(C$_3$H$_5$)(S,R,R-**1**)]SbF$_6$, **17**, was synthesized by Mezzetti and co-workers. These authors have kindly provided the X-ray data used in the DFT calculations. A manuscript from these authors concerning related compounds has been submitted to *Organometallics*.
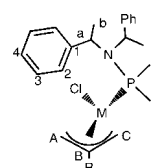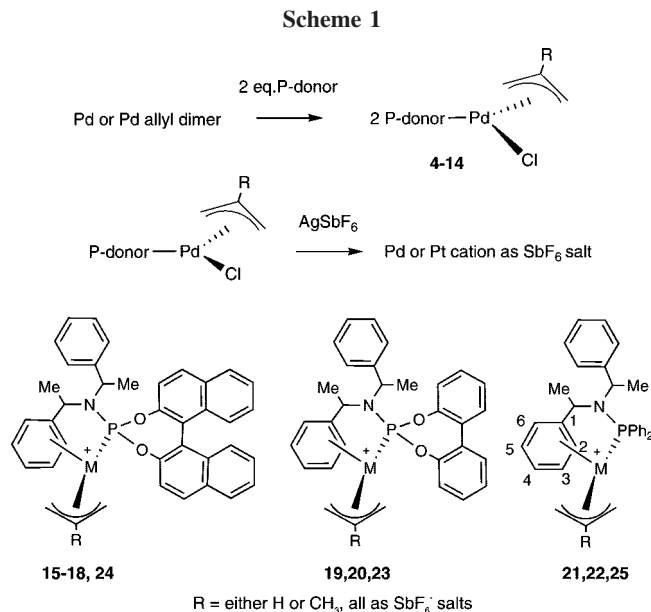
Scheme 1

R = either H or CH$_3$, all as SbF$_6^-$ salts

Table 1. ^{13}C NMR Chemical Shifts for Allyl and Selected Allyl and Aliphatic Resonances of the Chloro Compounds 4−14^a

complex		C$_a$	C$_b$	C1	C2	C$_A$	C$_C$	C$_C$
[PdCl(C$_3$H$_5$)(S,S,S-**1**)], **4**	major	55.2	21.4	142.1	129.0	79.5	119.1	58.4
	minor	55.1	21.7	141.9	129.1	78.8	118.1	58.8
[PdCl(C$_4$H$_7$)(S,S,S-**1**)], **5**	major	55.3	22.4	141.6	128.8	77.0	133.3	60.5
	minor	55.3	22.3	141.4	128.4	78.1	133.8	58.7
[PdCl(C$_3$H$_5$)(S,R,R-**1**)], **6**	major	53.9	20.3	143.1	128.5	78.5	nd	59.0
	minor	54.2	20.6	143.2	128.3	79.6	nd	57.8
[PdCl(C$_4$H$_7$)(S,R,R-**1**)], **7**	major	nd	20.5	143.4	nd	76.6	133.7	nd
	minor		19.7	142.8	nd	78.1	133.5	58.0
[PdCl(C$_3$H$_5$)(**2**)], **8**	major	54.0	20.6	142.8	128.9	78.9	118.2	58.9
	minor	54.3	21.0	142.7	128.6	79.3	119.1	57.7
[PdCl(C$_4$H$_7$)(**2**)], **9**	major	54.0	20.6	142.8	128.9	78.4	133.6	58.8
	minor	55.1	21.0	143.3	128.4	77.4	134.2	59.0
[PdCl(C$_3$H$_5$)(**3**)], **10**	major	nd	nd	nd	128.8	78.4	116.6	66.8
	minor		19.9	143.5	128.8	79.6	119.2	62.1
[PdCl(C$_4$H$_7$)(**3**)], **11**		56.4	20.1	143.8	128.9	76.2	131.9	67.3
[PtCl(C$_3$H$_5$)(S,R,R-**1**)], **12**	major	53.4	22.4	137.6	126.8	68.2	111.0	46.8
	minor	53.8	22.7	138.1	126.9	68.8	111.2	45.7
[PtCl(C$_3$H$_5$)(**2**)], **13**	major	54.2	20.4	142.8	128.6	67.9	110.2	46.1
	minor	54.6	20.6	143.0	128.4	68.7	110.0	45.3
[PtCl(C$_3$H$_5$)(**3**)], **14**	major	57.2	20.8	143.9	129.2	69.1	nd	51.9
	minor	57.2	20.8	144.0	129.2	69.4	nd	49.2

^{a} CD$_2$Cl$_2$, 500 or 700 MHz.

ligands. The substantial low-frequency shifts between ca. 15 and 40 ppm for carbons 1 and 2 in **23**−**25** are consistent with an η^2-olefin structure. For convenience we call these chemical shift changes "relative chemical shifts" rather than coordination chemical shifts. In some cases, e.g., for **24**, the ^{195}Pt satellites are observed as broad shoulders on the proton resonance H2 (see Figure 1). Unfortunately, due to fast CSA-induced relaxation,[17] this is not always the case. As expected the CH

(17) Efficient CSA relaxation is favored by both large B_0 fields (necessary for sufficient ^{1}H resolution) and low temperatures, which increase the solution viscosity and thus the correlation time, thereby decreasing T_1. The latter phenomenon is known as thermal decoupling.

**Table 2. ^{13}C NMR Chemical Shifts and Relative Chemical Shifts for Selected Allyl Resonances of the Cationic Compounds 15−25^a**

complex	C_A	$\Delta\delta$	C_B	$\Delta\delta$	C_C	$\Delta\delta$	T (K)
[Pd(C$_3$H$_5$)(S,S,S-1)]SbF$_6$, **15**	99.1, 95.4	18.1	120.9, 122.9	3.3	58.8, 62.6	2.1	173
[Pd(C$_4$H$_7$)(S,S,S-1)]SbF$_6$, **16**	98.0, 94.0	18.4	137.3,138.8	4.5	57.9, 62.3	0.5	173
[Pd(C$_3$H$_5$)(S,R,R-1)]SbF$_6$, **17**^{b}	97.8, 96.6	18.2	121.1, 122.3		57.4, 59.3	0.1	203
[Pd(C$_4$H$_7$)(S,R,R-1)]SbF$_6$, **18**	96.2, 93.4	17.4	137.7, 138.2	4.4	56.8, 60.1	0.4	203
[Pd(C$_3$H$_5$)(**2**)]SbF$_6$, **19**	96.6, 97.8	18.0	122.6, 121.3	3.3	59.4, 56.8	-0.2	193
[Pd(C$_4$H$_7$)(**2**)]SbF$_6$, **20**	96.0, 94.2	17.3	138.0, 138.8	4.5	57.3, 59.9	0.3	193
[Pd(C$_3$H$_5$)(**3**)]SbF$_6$, **21**	96.2, 94.0	15.6	122.0, 119.6	1.9	65.5, 61.2	-1.1	213
[Pd(C$_4$H$_7$)(**3**)]SbF$_6$, **22**	93.6	17.4	135.6	3.7	61.1	-6.3	213
[Pt(C$_3$H$_5$)(S,R,R-1)]SbF$_6$, **23**	85.9, 86.2	17.6	118.5	7.4	55.3, 51.8	7.3	298
[Pt(C$_3$H$_5$)(**2**)]SbF$_6$, **24**	91.3, 89.4	22.0	116.4,116.4	6.3	45.0, 46.8	0.2	253
[Pt(C$_3$H$_5$)(**3**)]SbF$_6$, **25**	87.2, nd	18.0	nd		53.2, nd	2.6	243

^{a} $\Delta\delta$ is relative to the chloro complexes. CD$_2$Cl$_2$ solutions, 500 or 700 MHz. ^{b} Synthesized by Mezzetti and co-workers (personal communication, manuscript in preparation).

resonance for C2 usually[18] experiences the largest change relative to the *ipso* C1. The chemical shift of C6 in **23**−**25** is only marginally affected.

Moving to the Pd salts, Figure 2 shows low-temperature spectra from two ^{13}C,^{1}H correlation spectra for Pd- salt **21**. One needs both the routine one-bond correlation to detect C2 and the long-range correlation (using $^3J(^{13}$C,^{1}H) via the methyl groups) to locate the *ipso* carbon, C1. The relative chemical shifts for these are not as large as for the Pt salts. This is partially related to the difference in back-bonding ability between Pt and Pd.

However, if the choice of temperature is not optimal,[19] the metal can slide across the π-donor and/or the olefin can dissociate and rotate around the C1−C(Me)N bond. This results

26
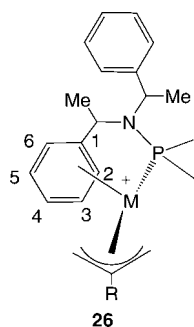
in some averaging of the relative shifts over both C2 and C6 (see eq 1 and Figure 3), thus decreasing the magnitude of the relative chemical shift for C2. This is clearly the case for almost, but not quite all of the Pd salts; see entries **15**, **16**, and **21** of
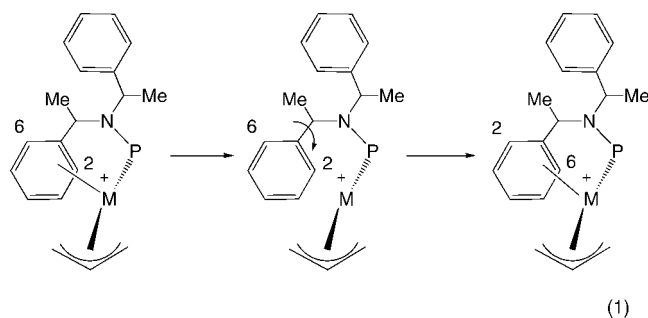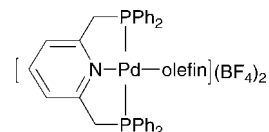

(1)

Table 3. For comparison, in Table 5, we show coordination chemical shifts for η²-olefin ligands in a model cationic

palladium species, shown below.[20] Our relative chemical shifts tend to be smaller than the coordination chemical shifts for this

chelating phosphine model, supporting the idea that our salts show only a weak interaction via the olefinic double bond. The new olefinic bonds are comparable to those found for palladium/MOP and ruthenium/phosphoramidites[12,13] (see Scheme 2).

The ^{1}H spectra for all of the salts do contain a potentially valuable hint with respect to the bonding. One observes two very different $^3J(^{31}$P,^{1}H) values for the two amino side-chain methine CH protons. A representative selection of values is presented in Table 6. The unusually large $^3J(^{31}$P,^{1}H) value of 39−42 Hz is associated with the complexed arm and most probably stems from an enforced conformation due to the olefin complexation. Molecular models in addition to a solid-state structure[21] suggest that the P−N−C−H dihedral angle is close to 180° (161° from DFT calculations; see the structure


Structure fragment
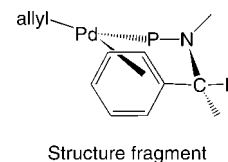
fragment), so that the observed vicinal coupling constant corresponds to about the maximum expected assuming a literature Karplus relationship.[22] The changes in the values for $^3J(^{31}$P,^{1}H) for the noncomplexed phenylethyl side chain depend on the nature of the ligand (compare the values for **19** and **20** using ligand **2** as well as those for **18** and **23** using S,R,R-**1**).

The ^{13}C chemical shifts for the terminal *allyl* positions are presented in Tables 1 and 2. All of the neutral chloro-palladium[23] compounds **4**−**11** show chemical shifts in the range (a) 76−80 ppm for the position pseudo-*trans* to the P-donor, C_A, and (b) 58−67 ppm for the allyl carbons pseudo-*trans* to

---

(18) For the salt containing the biphenol-based ligand, **2**, this sequence is reversed.
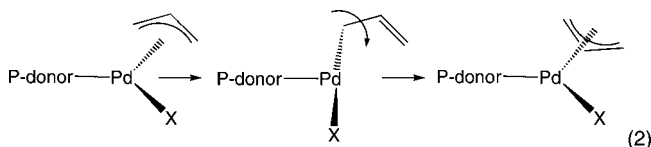
chloride, C_C. These chemical shifts are consistent with those of the model compounds **27**,[24] **28**,[25] and **29**,[26] containing phosphines or a carbene.
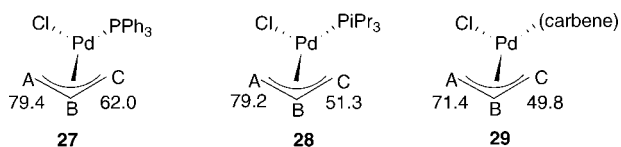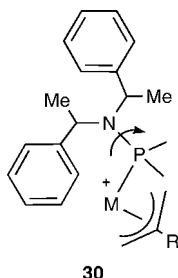

For the palladium cationic series **15**−**22** (see Table 2), the chemical shifts for C_A fall in the range 93−99 ppm, while for C_C values lie between 57 and 66 ppm. Consequently, substitution of the chloride by the η^2-olefin results in a high-frequency chemical shift of the carbon atom *trans* to the phosphorus ligand, C_A, while C_C experiences no substantial change. These values are somehow surprising, since one might have expected a larger effect on the allyl carbon, C_C, located in *trans* position to the new ligating group. Perhaps the steric effects associated with the complexed olefin help to weaken the bonding to C_A.

This brings us to the various possible dynamics in these salts. One can envision at least four intramolecular processes:

1. The frequently reported[27] η^3−η^1−η^3 isomerization mechanism, which can proceed by several mechanisms (only one of which is shown in eq 2) and may be rather selective.

2. Rotation around the P−N bond, as indicated in **30**, which will exchange the positions of the two amino side-chain phenyl groups.

30

3a. Rotation around the C(phenyl)−CH(Me)N bond, which process, e.g., after dissociation of the complexed olefin, exchanges the H2 and H6 protons; see eq 1.

3b. The same net result, i.e., exchange of the *ortho* positions on the phenyl ring, can be obtained if the metal "slides" or "jumps" from C1−C2 to the neighboring C1−C6.

Figure 3 shows a set of variable-temperature ^{1}H measurements for **19**. These spectra reveal that the allyl protons are relatively sharp at ambient temperature. Exchange may still be present, but it will most likely not be faster than a few per second (i.e., close to the line widths). At ambient temperature one does not easily find the side-chain CH signals, but these do become relatively sharp at ca. 233 K and are found at $\delta = 4.3$ and 4.9 ppm. Clearly process 2 has a lower activation energy than the allyl isomerization. Further, as indicated by the line shapes, the "H2, H6" exchange (process 3) is still proceeding even at 213 K (see the shapes of the signals between 6.0 and 6.5 ppm). The 2D exchange map of the same compound, at 213 K, confirms this assumption, as shown in Figure 4. Although most of the aromatic protons are strongly overlapped, the *ortho* H2 resonances are resolved and the cross-peaks for the exchange with H6 readily visible. The figure also shows the exchange between the *meta* protons, and these signals can be seen at higher frequencies (see Figure 4, between 7.5 and 7.9 ppm). The aliphatic part of the exchange map (not shown in the figure) reveals that the exchange processes for the methyl and methine groups of the ligand are slow at this temperature, but still present, as suggested by the line shapes. Consequently, the activation energies for processes 2 and 3a/3b, in **19**, are not very different, although the 3a/3b processes have a slightly lower energy barrier.

However, the exchange data from Figure 5 for **21** provide support for the contention that both process 2 and process 3a/3b can have similar activation energies. In this spectrum the two amino-methyl phenyl rings are exchanging within both isomers. The two, now equivalent, protons, Hc (from the noncoordinated side chain of the two isomers), are exchanging with the two *ortho* protons, Ha and Hb, from the coordinated ring, due to rotation around the P−N bond. The protons Ha and Hb are in exchange due to rotation of the complexed ring

(19) This is not a trivial choice since, at lower temperatures, one begins to observe restricted rotation around the various C−C and, for the SimplePhos, **3**, P−C bonds, with the resultant loss of resolution and spectral clarity. At higher temperatures, the dynamics of olefin exchange dominate. Consequently, the temperatures indicated represent the most reasonable compromise possible. On the basis of the observed temperature-dependent line shapes we estimate an activation energy of ca 10−13 kcal mol^{-1}.

(20) Hahn, C.; Morvillo, P.; Vitagliano, A. *Eur. J. Inorg. Chem.* **2001**, (2), 419−429.

(21) Personal communication from A. Mezzetti, ETHZ, 2007.

(22) Bentrude, W. G.; Setzer, W. N. In *Phosphorus-31 NMR Spectroscopy in Stereochemical Analysis−Organic Compounds and Metal Complexes*; Verkade, J. G., Quin, L. D., Eds.; VCH: Deerfield Beach, FL, 1987.

(23) The chloro compounds show ^{13}C chemical shifts in the range 68−70 ppm for C_A and 45−52 ppm for C_C. For the cationic compounds C_A has a δ between 86 and 91 ppm, while the chemical shift for C_C is in the range 45−55 ppm.

(24) Shaw, B. L.; Mann, B. E.; Pietropaolo, R. *Chem. Commun.* **1971**, (15), 790−791.

(25) Krause, J.; Goddard, R.; Mynott, R.; Poerschke, K.-R. *Organometallics* **2001**, *20* (10), 1992−1999.

(26) Viciu, M. S.; Germaneau, R. F.; Navarro-Fernandez, O.; Stevens, E. D.; Nolan, S. P. *Organometallics* **2002**, *21* (25), 5470−5472.
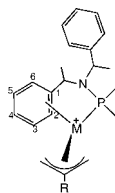
(27) (a) Vrieze, K. In *Dynamic Nuclear Magnetic Resonance Spectroscopy*; Jackman, L. M., Cotton, F. A., Eds.; Academic Press: New York, 1975; pp 441−483. (b) Pregosin, P. S.; Albinati, A.; Rizzato, S. *Organometallics* **2006**, *25*, 5955–5964. (c) Pregosin, P. S.; Salzmann, R. *Coord. Chem. Rev.* **1996**, *155*, 35–68. (d) Herrmann, J.; Pregosin, P. S.; Salzmann, R.; Albinati, A. *Organometallics* **1995**, *14* (7), 3311–3318. (e) Pregosin, P. S.; Salzmann, R.; Togni, A. *Organometallics* **1995**, *14*, 842. (f) Breutel, C.; Pregosin, P. S.; Salzmann, R.; Togni, A. *J. Am. Chem. Soc.* **1994**, *116* (9), 4067–4068. (g) Burckhardt, U.; Gramlich, V.; Hofmann, P.; Nesper, R.; Pregosin, P. S.; Salzmann, R.; Togni, A. *Organometallics* **1996**, *15*, 3496–3503. (h) Togni, A.; Burckhardt, U.; Gramlich, V.; Pregosin, P. S.; Salzmann, R. *J. Am. Chem. Soc.* **1996**, *118* (5), 1031–1037. (i) Cesarotti, E.; Grassi, M.; Prati, L.; Demartin, F. *J. Chem. Soc., Dalton Trans.* **1991**, 2073. (j) Mandal, S. K.; Gowda, G. A. N.; Krishnamurthy, S. S.; Zheng, C.; Li, S. J.; Hosmane, N. S. *Eur. J. Inorg. Chem.* **2002**, (8), 2047–2056. (k) Mandal, S. K.; Gowda, G. A. N.; Krishnamurthy, S. S.; Nethaji, M. *Dalton Trans.* **2003**, (5), 1016–1027. (l) Crociani, B.; Antonaroli, S.; Bandoli, G.; Canovese, L.; Visentin, F.; Uguagliati, P. *Organometallics* **1999**, *18* (7), 1137–1147. (m) Crociani, B.; Antonaroli, S.; Paci, M.; Di Bianca, F.; Canovese, L. *Organometallics* **1997**, *16*, 384–391. (n) Gogoll, A.; Ornebro, J.; Grennberg, H.; Bäckvall, J. E. *J. Am. Chem. Soc.* **1994**, *116*, 3631. (o) Sprinz, J.; Kiefer, M.; Helmchen, G.; Reggelein, M.; Huttner, G.; Zsolnai, L. *Tetrahedron Lett.* **1994**, *35*, 1523–1526. (p) Kollmar, M.; Helmchen, G. *Organometallics* **2002**, *21* (22), 4771–4775. (q) Faller, J. W.; Wilt, J. C. *Organometallics* **2005**, *24* (21), 5076–5083. (r) Faller, J. W.; Sarantopoulos, N. *Organometallics* **2004**, *23* (9), 2179–2185. (s) Faller, J. W.; Wilt, J. C.; Parr, J. *Org. Lett.* **2004**, *6* (8), 1301–1304. (t) Faller, J. W.; Stokes-Huby, H. L.; Albrizzio, M. A. *Helv. Chim. Acta* **2001**, *84* (10), 3031–3042. (u) Lloyd-Jones, G. C.; Stephen, S. C.; Murray, M.; Butts, C. P.; Vyskocil, S.; Kocovsky, P. *Chem.−Eur. J.* **2000**, *6*, 4348–4357.

Table 3. ^{13}C Data and Relative Chemical Shifts for C1, C2, and C6 for the Salts^a

				site				
complex		C1	$\Delta\delta$	C2	$\Delta\delta$	C6	$\Delta\delta$	T (K)
[Pd(C$_3$H$_5$)(S,S,S-**1**)]SbF$_6$, **15**	major	131.9	−10.1	111.8	−17.2	123.9	−5.2	173
	minor	133.3	−8.7	106.6	−22.4	127.4	−1.6	
[Pd(C$_4$H$_7$)(S,S,S-**1**)]SbF$_6$, **16**	major	131.3	−10.2	110.8	−17.8	125.0	−3.6	173
	minor	131.5	−10.0	106.3	−22.3	127.8	−0.8	
[Pd(C$_3$H$_5$)(S,R,R-**1**)]SbF$_6$, **17**^{b}	major	132.9	−10.2	115.2	−13.2	121.0	−7.4	203
	minor	131.8	−11.4	113.0	−15.4	117.5	−10.9	
[Pd(C$_4$H$_7$)(S,R,R-**1**)]SbF$_6$, **18**	major	131.4	−11.6	113.7	−14.7	118.0	−10.4	203
	minor	133.3	−9.8	116.2	−12.2	117.7	−10.7	
[Pd(C$_3$H$_5$)(**2**)]SbF$_6$, **19**	major	133.4	−9.4	111.2	−17.6	122.6	−6.2	193
	minor	134.1	−8.6	113.8	−15.0	119.1	−9.6	
[Pd(C$_4$H$_7$)(**2**)]SbF$_6$, **20**	major	128.9	−14.2	114.4	−14.2	119.5	−9.2	193
	minor	128.4	−14.6	114.1	−14.6	117.8	−10.9	
[Pd(C$_3$H$_5$)(**3**)]SbF$_6$, **21**	major	133.1	−10.4	103.8	−25.0	127.8	−1.0	213
	minor	132.9	−10.6	104.6	−24.2	127.4	−1.4	
[Pd(C$_4$H$_7$)(**3**)]SbF$_6$, **22**		133.7	−10.1	nd		nd		213
[Pt(C$_3$H$_5$)(S,R,R-**1**)]SbF$_6$, **23**	major	113.8	−24.0	88.0	−38.8	ca. 127	ca. 0.2	298
	minor	116.0	−21.8	87.4	−39.4	ca. 127	ca. 0.2	
[Pt(C$_3$H$_5$)(**2**)]SbF$_6$, **24**	major	122.9	−21.0	113.4	−15.1	ca. 128	ca. −0.5	253
	minor	125.7	−18.2	109.3	−19.2	ca. 128	ca. −0.5	
[Pt(C$_3$H$_5$)(**3**)]SbF$_6$, **25**	major	122.6	−21.4	103.6	−25.6	123.1	−6.1	243
	minor	nd		nd		nd		

^{a} $\Delta\delta$ is relative to the chloro complexes. CD$_2$Cl$_2$ solutions, 500 or 700 MHz. ^{b} Synthesized by Mezzetti and co-workers (personal communication, manuscript in preparation).

around the C(aryl)−CH(Me)N bond. Note that the two Hc resonances are *not in exchange* with each other. Since the allyl interconversion is slow at this temperature, the spectrum shows two independent sets of cross-peaks, one for each allyl arrangement.

In terms of relative rates of the two processes as a function of the P-donor, it seems that for phosphoramidite-type auxiliaries (ligands **1** and **2**) process 3 possesses the lowest activation energy. On the other hand for aminophosphine-type ligand **3**, the exchange of the complexed and free side chains has a relatively lower energy barrier. These observations are qualitative and based on the relative intensities of the exchange cross-peaks.

The chirality of phosphoramidites, as discussed in the Introduction, arises from two modular elements: the atropoisomeric backbone and the stereogenic centers within the chiral amine. From catalysis results[4,18,28−30] it is known that only one diastereomeric combination affords high enantioselectivities, the so-called matched series, and it is assumed that the binaphthol unit is imposing the absolute stereochemistry of the catalytic product. When flexible binol backbones are used, the amine alone is sufficient to induce atropoisomerism.[28] Since the two diastereomeric complexes from **1** should show different structures, we had hoped to detect differences in the olefin coordination via the ^{13}C data. Unfortunately different temperatures were necessary for the analysis of the two series of compounds

(28) Feringa, B. L.; Pineschi, M.; Arnold, L. A.; Imbos, R.; De Vries, A. H. M. *Angew. Chem., Int. Ed. Engl.* **1997**, *36* (23), 2620–2623.

(29) (a) Knöbel, A. K. H.; Escher, I. H.; Pfaltz, A. *Synlett* **1997**, (12), 1429–1431. (b) Escher, I. H.; Pfaltz, A. *Tetrahedron* **2000**, *56* (18), 2879–2888.

(30) Alexakis, A.; Rosset, S.; Allamand, J.; March, S.; Guillen, F.; Benham, C. *Synlett* **2001**, *9*, 1375–1378.

15−18, so that the ^{13}C results are not readily interpreted. In any case, it is not obvious that these relative chemical shifts are very different.

DFT calculations were performed for the Pd complex [Pd(C$_3$H$_5$)(S,R,R-**1**)]$^+$ (using the crystallographic data from **17**)[16,21] and (given the interest in related ruthenium chemistry, namely, the fact that a similar bond was observed in a Ru complex bearing different chiral ligands) a model RuCl(p-cymene) complex (**Ru**) depicted in Figure 6 (right side),[12] where the naphthyl group was replaced by the biaryl analogue.

The structures of the complexes were fully optimized, and an energy partitioning analysis was carried out (see Experimental Section for details). Two alternative structures, **17*** and **Ru***, with enforced long distances between the metal and all phenyl groups, were optimized as well, and all four structures are shown in Figure 6. This methodology is similar to that described in an earlier publication.[8]

A third structural possibility was considered in which the phenyl groups of the amine side chain were kept far from the metal, and a proximate double bond of the naphthyl fragment was allowed to approach either the Ru or the Pd. No low-energy structure with an η^2-olefin could be obtained.

The calculated structure of the Pd complex **17** is very close to the experimental one. Specifically, the Pd−C distances to the weakly bound phenyl carbon atoms are 2.445 and 2.477 Å, whereas the experimental values are 2.413 and 2.514 Å. The agreement is not quite as good in the Ru complex (calculated: 2.497, 2.477 Å; experimental: 2.386, 2.378 Å), possibly because the model complex chosen is different from the complex for which one has X-ray data.

In the alternative "nonbonded" structure containing Pd, **17***, where no weak η^2 interaction occurs, the shortest Pd−C distance involving the amine phenyl groups is 3.617 Å. Interestingly, in

Table 4. ^{31}P NMR Data and Relative Chemical Shifts for the Cationic Compounds (all of the data refer to CD$_2$Cl$_2$ solutions, 500 or 700 MHz)

|	isomer		
complex	major	minor	$\Delta\delta$
[Pd(C$_3$H$_5$)(*S,S,S*-**1**)]SbF$_6$, **15**	151.9	153.3	2.2
[Pd(C$_4$H$_7$)(*S,S,S*-**1**)]SbF$_6$, **16**	151.6	152.4	1.1
[Pd(C$_3$H$_5$)(*S,R,R*-**1**)]SbF$_6$, **17**	148.1	148.8	1.1
[Pd(C$_4$H$_7$)(*S,R,R*-**1**)]SbF$_6$, **18**	148.2	149.6	1.0
[Pd(C$_3$H$_5$)(**2**)]SbF$_6$, **19**	148.8	149.4	0.5
[Pd(C$_4$H$_7$)(**2**)]SbF$_6$, **20**	149.1	150.6	0.9
[Pd(C$_3$H$_5$)(**3**)]SbF$_6$, **21**	84.2	84.3	32.8
[Pd(C$_4$H$_7$)(**3**)]SbF$_6$, **22**	84.8		34.6
[Pt(C$_3$H$_5$)(*S,R,R*-**1**)]SbF$_6$, **23**^{a}	137.8	138.0	−4.9
[Pt(C$_3$H$_5$)(**2**)]SbF$_6$, **24**^{b}	141.6	141.7	6.0
[Pt(C$_3$H$_5$)(**3**)]SbF$_6$, **25**^{c}	82.1	82.2	27.6

^{a} ^1J(Pt,P) = 6827 Hz (major), 4655 Hz (minor); ^{195}Pt δ = −5101 (major), −5080 (minor). ^{b} ^1J(Pt,P) = 7114 Hz (major), 7056 Hz (minor); ^{195}Pt δ = −4942 (major), −4988 (minor). ^{c} ^1J(Pt,P) = 4565 Hz (major), 4655 Hz (minor).
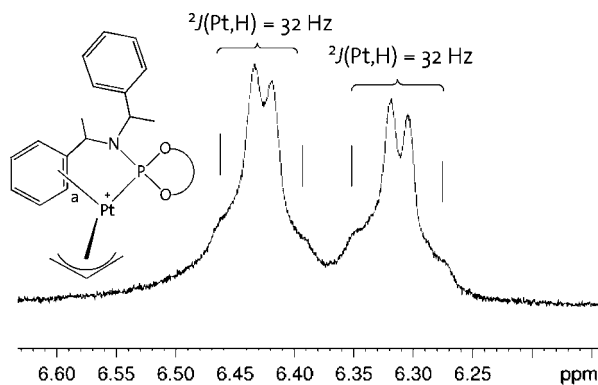
Figure 1. Section of the ^{1}H spectrum of Pt salt **24** showing the complexed two aryl C-H2 protons (from the two isomers) with their broad ^{195}Pt satellites.
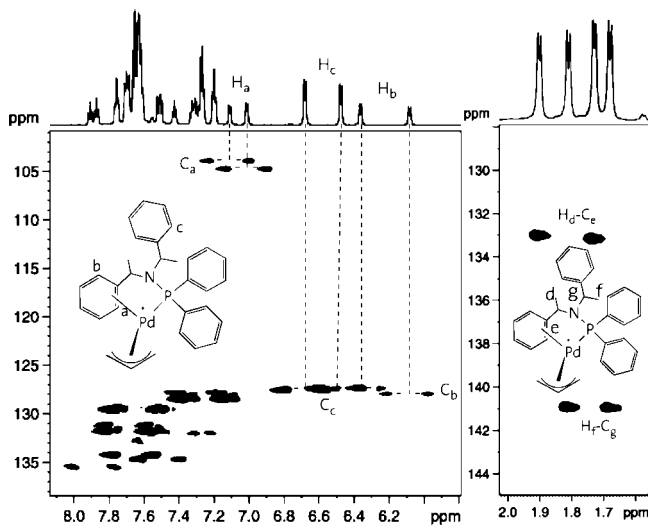
Figure 2. Sections of two ^{13}C,^{1}H correlations for **21**: (left) the one-bond correlation showing the two aryl C2 CH resonances of both isomers at ca. 104 ppm and (right) the result from the long-range correlation (using the methyl groups and their ^3J(C,H) values) showing the positions of the four C1 phenyl *ipso* carbons. Two of these C1 signals, at ca. 133 ppm, are shifted to lower frequency by ca. 8 ppm.

the Ru model complex, **Ru***, there is a short contact (3.315 Å) and it involves the biaryl (binol) group of the phosphine. Figure 6 also provides the relevant M−C distances for these four
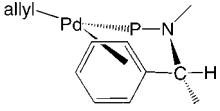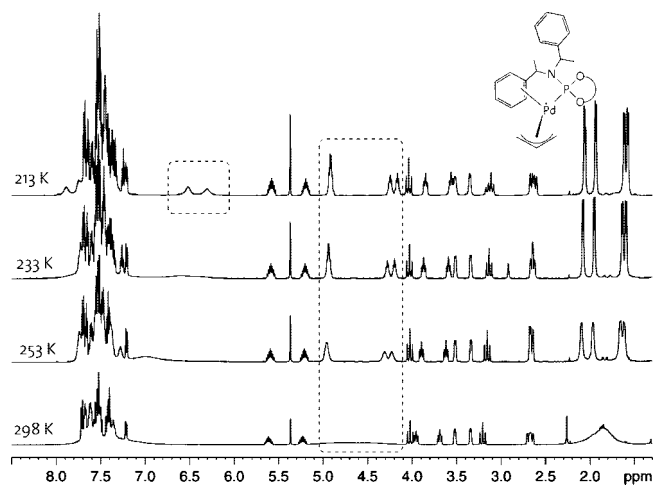

Figure 3. Series of variable-temperature ^{1}H NMR spectra for complex **19**. Note that the side-chain CH and CH$_3$ signals are broad at ambient temperature, but that the allyl resonances are relatively sharp.

Table 5. ^{13}C NMR Data and Coordination Chemical Shifts for Selected Olefins in a Model Complex^{35}

olefin	δ(=CH$_2$)	$\Delta\delta$(=CH$_2$)	δ(=CH)	$\Delta\delta$(=CH)
CH$_2$=CH$_2$	88.0	−35.3		
MeCH=CH$_2$	86.4	−29.6	118.1	−16.5
PHCH=CH$_2$	77.2	−34.8	120.2	−15.3
(*Z*)-MeCH=CHMe			110.9	−14.4
(*E*)-MeCH=CHMe			107.8	−17.6
norbornene			105.2	−30.5

Scheme 2

C1 = -7.6 ppm
C2 = -23.7 ppm

C1 = -24.3 ppm
C2 = -22.4 ppm
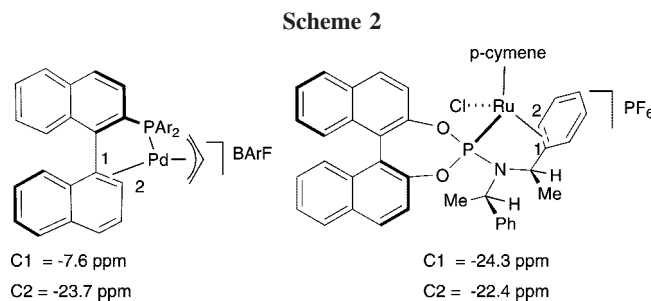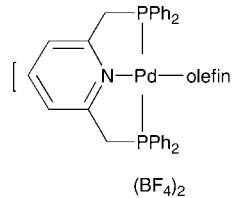
structures (and two tables of Supporting Information, S1 and S2 provide more detail). These short contact distances for **17*** and **Ru*** are too long to be considered covalent bonds; however, we shall use these results to represent the nonbonding counterparts of complexes **17** and **Ru**, respectively.

Mayer indices (MI) were used as bond strength indicators to confirm the trends given by the distances. In the Pd complex **17**, the MIs for the η^2-interactions are 0.249 and 0.296, while for the three allyl Pd−C bonds they range from 0.254 (central) to 0.437 and 0.568. The value for the Pd−P bond is 0.982. In complex **17***, the strength of the bonds to the allyl carbon atoms stays the same (central: 0.253) or becomes stronger (terminal carbons: 0.441, 0.631). Although the Pd−P bond index barely changes (0.967), the index for the long interaction (3.617 Å) is very small (0.034). This value is ∼8−9 times smaller than the effective Pd−C η^2-interactions and can be neglected.

Table 6. $^3J(P,H)$ Values for the Phenylethyl Groups of Selected Complexes

	$^3J(^{31}P,^1H)$	
complex	complexed arm	free arm
[Pd(C$_3$H$_5$)(S,S,S-**1**)]SbF$_6$, **15**	41	nd
[Pd(C$_4$H$_7$)(S,S,S-**1**)]SbF$_6$, **16**	41, 42	ca. 19
[Pd(C$_4$H$_7$)(S,R,R-**1**)]SbF$_6$, **18**	41	ca. 7
[Pd(C$_3$H$_5$)(**2**)]SbF$_6$, **19**	40	ca. 14
[Pd(C$_4$H$_7$)(**2**)]SbF$_6$, **20**	41	ca. 13
[Pd(C$_4$H$_7$)(**3**)]SbF$_6$, **22**	39	nd
[Pt(C$_3$H$_5$)(S,R,R-**1**)]SbF$_6$, **23**	39	ca. 7

The situation is similar in the Ru model complexes. In **Ru**, the relevant MIs are as follows: Ru−Cl (0.824), Ru−P (1.057), Ru−C1 (0.326), Ru−C2 (0.267). For **Ru*** these change to Ru−Cl (0.869), Ru−P (0.817), and Ru−C(arene carbon at 3.315 Å) 0.008. The Ru−C bonds to the carbon atoms in the *p*-cymene ring become stronger in **Ru*** (0.334, 0.351, 0.401, 0.418, 0.448, 0.454, compared to 0.309, 0.335, 0.365, 0.415, 0.440, 0.461 in **Ru**). Again, the strength of the presumed Ru−C weak interaction in **Ru*** is negligible compared to the two existing interactions in the initial structure of **Ru**. Interestingly the Ru−P bond also weakens, probably because of the distortion imposed to the ligand. The metal makes stronger bonds only to Cl and the ring in *p*-cymene. Wiberg indices can be used for the same purpose (these are given in Tables S1 and S2) and give the same qualitative information with respect to the bond strengths.

In order to estimate the strength of the Pd−C η^2-interactions, we carried out an energy decomposition analysis (see Experimental Section for details), and the results are collected in Table 7. The first surprising result concerns the strength of the η^2-arene interaction (30.13 kcal mol^{-1}) for the Ru complex **17**. The corresponding value in the Pd complex (12.94 kcal mol^{-1}) approaches the values calculated in a previous study involving [CpMo(CO)$_2$(PPh$_3$)]$^+$ (8.58 kcal mol^{-1}) and [CpRu(Binap)]$^+$ (13.74 kcal mol^{-1}).[8]

The reorganization energies of the two fragments between the two geometries are small, close to 0 for the metal fragment [Pd(allyl)]$^+$ or [Ru(*p*-cymene)Cl]$^+$, and not much larger for the

ligand. The [Pd(allyl)]$^+$ moiety is slightly less stable (0.03 kcal mol^{-1}) when the C=C bond is not coordinated, the opposite taking place for Ru. When the differences for the other contributions in both geometries (**17** and **17***) are examined for the Pd complex, the electrostatic and Pauli terms practically cancel each other (−15.38, 17.21), with the binding energy ΔE (−12.66 kcal mol^{-1}) being almost the same as the orbital term (ΔE_{orb}= −12.94 kcal mol^{-1}).

The situation is different for the Ru complex. The electrostatic term ΔE_{elec} drops by 85.46 kcal mol^{-1} when varying the coordination sphere of the metal and is accompanied by a large loss of orbital interaction (56.06 kcal mol^{-1}). As the Pauli repulsion (ΔE_{pauli}) decreases by a relatively large amount (103.64), the global result reveals a large interaction energy between the C=C bond of the amine phenyl and the Ru fragment (30.13 kcal mol^{-1}).

Comparing this situation with the one described earlier for [CpRu(Binap)]$^+$, one finds that the major difference involves the ready ability of the amine side chain in the **Ru** complex to approach the metal; that is, this fragment does not need to distort in order to complex. This fact is reflected in the low change of reorganization energy, 6.02 kcal mol^{-1}. This was not the case in [CpRu(Binap)]$^+$, where the reorganization energy of Binap was 19.45 kcal mol^{-1}, a factor that largely contributed to the weak η^2-arene interaction (the lower Mayer indices confirm this aspect). Notice that a similar approach of the naphthyl fragment in the ligand is almost impossible in **Ru**, owing to the presence of the oxygen atom. In the absence of large preparation energies, the η^2-arene interaction cannot even be called weak. The distances and MIs involved are comparable to those observed between Ru and the *p*-cymene carbon atoms.

In the known 16-electron species [CpMo(CO)$_2$(PPh$_3$)]$^+$, the interaction with a C=C bond helps to decrease the electronic unsaturation (large ΔE_{orb}); on the other hand, the coordination number rises to seven and other effects compensate, leading to a very weak interaction.

The calculated change in ^{13}C chemical shifts associated with the relevant carbon atoms also shows clearly a different behavior exhibited by the carbon atoms involved in the weak bond (Table S3).

Conclusions

Incorporation of two chiral α-phenethyl amine side chains into the P-donor ligands places one of the two phenyl groups in a position to interact with the Pd and Pt centers in our cationic allyl complexes. Both the NMR data and the DFT calculations suggest that the binding energies in the η^2-olefin cationic complexes that form are relatively low (∼13 kcal mol^{-1}), in agreement with the fluxional behavior observed. However this type of weak bond is interesting in that it may be sufficient to briefly stabilize a coordinatively unsaturated metal complex and/ or a reactive transition state.

Experimental Section

General Procedures. All reactions and manipulations were performed under a N$_2$ atmosphere using standard Schlenk techniques. The palladium precursors [Pd(C$_3$H$_5$)Cl]$_2$ and [Pd(C$_4$H$_7$)Cl]$_2$ and the silver salts were purchased from commercial sources and used as received from the producer. Silver salts were stored in a glovebox. Phosphoramidite ligands **1**, **2**, and SimplePhos,[3] **3**, and complexes of the type [Pd(allyl)(phosphoramidite)Cl][4] were synthesized according to published procedures. Solvents were dried
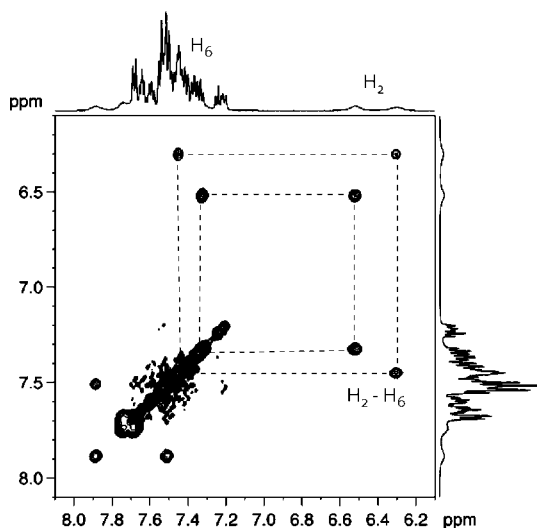

Figure 4. 2D exchange spectrum for **19** showing the "H2, H6" exchange for the two isomers. The H6 resonances are strongly overlapped.
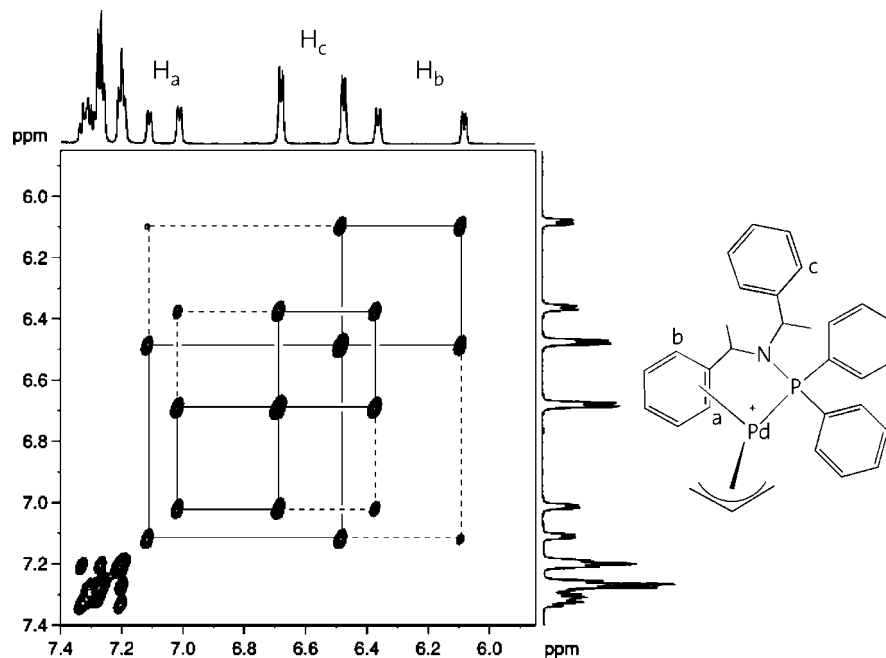
Figure 5. 2D NOESY spectrum of **21** showing that the two amino-methyl phenyl rings are exchanging in both isomers. The two equivalent protons, Hc (from the two isomers), are exchanging with the two *ortho* protons, Ha and Hb, from the other ring due to rotation around the P–N bond. The protons Ha and Hb are in exchange due to processes 3a,b. The two Hc resonances are not in exchange with each other, as the allyl interconversion is slow at this temperature.
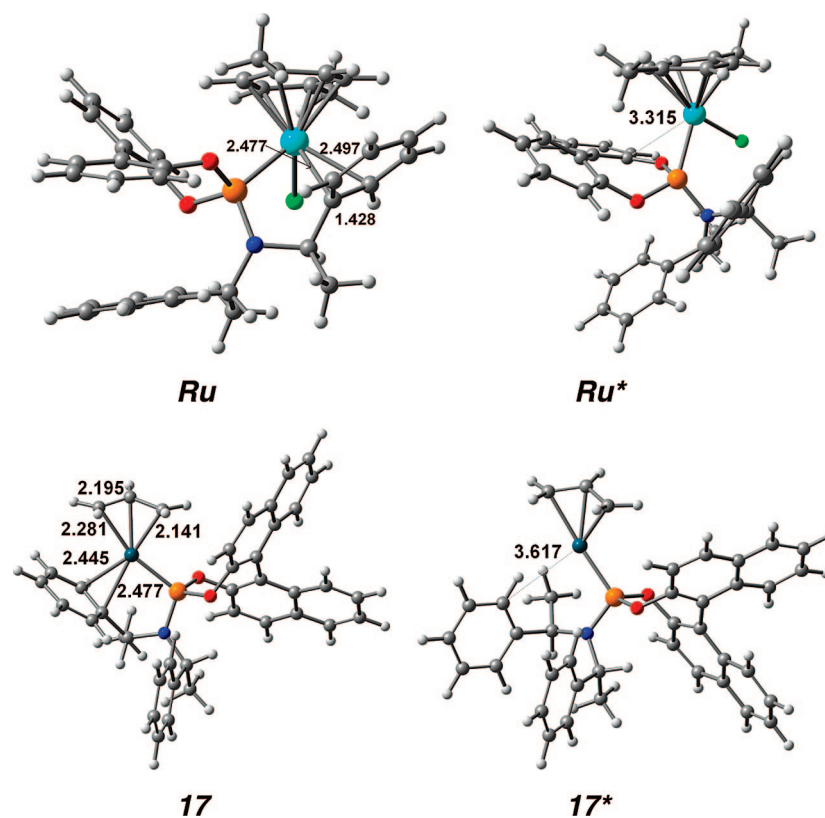

Figure 6. DFT-optimized structures for the complexes **17**, **17***, **Ru**, and **Ru***, emphasizing the shortest M–C contacts with phenyl groups.

and distilled under standard procedures and stored under nitrogen. NMR spectra were recorded with Bruker DPX-250, 300, 400, 500, and 700 MHz spectrometers at room temperature, unless otherwise stated. Chemical shifts are given in ppm; coupling constants (J) in hertz. Elemental analyses and mass spectroscopic studies were performed at the ETHZ. Extensive lists of detailed NMR data can be found in supplementary tables S4–S14.

Synthesis of [PdCl(allyl)(phosphoramidite)]. A solution of the P-donor ligand (0.180 mmol, 2.0 equiv) in CH_2Cl_2 (5 mL) is slowly added, under stirring, to a solution of the suitable dinuclear species [Pd(μ-Cl)(allyl)]$_2$ (0.090 mmol, 1.0 equiv) in CH_2Cl_2 (5 mL). After the addition is finished, the solution is stirred for 15 min, then the solvent is removed under reduced pressure, giving a solid, which is washed with diethyl ether and dried under vacuum.

Table 7. Energy Decomposition^a for the Interaction between L and M in [Pd(C₃H₅)(1)]⁺ (17) and a Model of [Ru(p-cymene)Cl(1)]⁺ (Ru)

	17	17*	Δ (17−17*)	Ru	Ru*	Δ (Ru−Ru*)
E_{prep}(L)	8.89	11.03	−2.14	19.76	13.74	6.02
E_{prep}(M)	2.66	2.63	0.03	11.10	10.36	0.74
ΔE_{prep}	**11.55**	**13.66**	**−2.11**	**30.86**	**24.10**	**6.76**
ΔE_{elec}	−150.83	−135.45	−15.38	−174.11	−89.65	−85.46
ΔE_{pauli}	167.21	150.00	17.21	228.19	124.55	103.64
ΔE_{orb}	−107.83	−95.17	−12.66	−147.91	−91.85	−56.06
ΔE_{int}	**−91.45**	**−80.62**	**−10.83**	**−93.83**	**−56.94**	**−36.89**
Δ$E = −D_e$	**−79.90**	**−66.96**	**−12.94**	**−62.97**	**−32.84**	**−30.13**

^{a} Values in kcal mol⁻¹; L = ligand **1** and M = [Pd(allyl)]⁺ (**17, 17***) or L = small ligand **1(1′)** and M = [Ru(p-cymene)Cl]⁺ (**Ru, Ru***).

[PdCl(C₃H₅)(S,S,S-1)], 4: white solid, yield 90%. Anal. Calcd for C₃₉H₃₅ClNO₂PPd: C, 64.83; H, 4.88; N, 1.94. Found: C, 63.95; H, 4.92; N, 1.90. MALDI MS: 1184 (M⁺ − Cl − C₃H₅ + L), 686 (M⁺ − Cl), 645 (M⁺ − Cl − C₃H₅), 538 (M⁺ − Cl − C₃H₅ − Pd).

[PdCl(C₄H₇)(S,S,S-1)], 5: yellowish-white solid, yield 95%. Anal. Calcd for C₄₀H₃₇ClNO₂PPd: C, 65.23; H, 5.06; N, 1.90. Found: C, 64.42; H, 5.16; N, 1.90. MALDI MS: 700 (M⁺ − Cl), 644 (M⁺ − Cl − CH₂CCH₃CH₂), 538 (M⁺ − Cl − CH₂CCH₃CH₂ − Pd).

[PdCl(C₄H₇)(S,R,R-1)], 6: white solid, yield 91%. Anal. Calcd for C₄₀H₃₇ClNO₂PPd · H₂O: C, 63.64; H, 5.20; N, 1.86. Found: C, 63.34; H, 5.19; N, 2.01. MALDI MS: 700 (M⁺ − Cl), 645 (M⁺ − Cl − CH₂CCH₃CH₂), 538 (M⁺ − Cl − CH₂CCH₃CH₂ − Pd).

[PdCl(C₃H₅)(2)], 8: white solid, yield 92%. Anal. Calcd for C₃₁H₃₁ClNO₂PPd · H₂O: C, 58.14; H, 5.19; N, 2.18. Found: C, 58.70; H, 5.09; N, 2.21. MALDI MS: 984 (M⁺ − Cl − C₃H₅ + L), 586 (M⁺ − Cl), 545 (M⁺ − Cl − C₃H₅), 440 (M⁺ − Cl − C₃H₅ − Pd).

[PdCl(C₄H₇)(2)], 9: white solid, yield 93%. Anal. Calcd for C₃₂H₃₃ClNO₂PPd: C, 60.39; H, 5.23; N, 2.20. Found: C, 60.40; H, 5.19; N, 2.40. MALDI MS: 600 (M⁺ − Cl), 545 (M⁺ − Cl − CH₂CCH₃CH₂), 438 (M⁺ − Cl − CH₂CCH₃CH₂ − Pd).

[PdCl(C₃H₅)(3)], 10: pale green solid, yield 90%. Anal. Calcd for C₃₁H₃₃ClNO₂PPd · H₂O: C, 60.99; H, 5.77; N, 2.29. Found: C, 60.72; H, 5.49; N, 2.25. MALDI MS: 556 (M⁺ − Cl), 515 (M⁺ − Cl − C₃H₅), 410 (M⁺ − Cl − C₃H₅ − Pd).

[PdCl(C₄H₇)(3)], 11: pale green solid, yield 92%. Anal. Calcd for C₃₂H₃₅ClNO₂PPd · H₂O: C, 61.54; H, 5.97; N, 2.24. Found: C, 60.80; H, 5.71; N, 2.24. MALDI MS: 570 (M⁺ − Cl), 515 (M⁺ − Cl − CH₂CCH₃CH₂), 410 (M⁺ − Cl − CH₂CCH₃CH₂ − Pd).

Synthesis of [Pd(allyl)(phosphoramidite)]SbF₆ (NMR sample). A solution of the suitable [PdCl(C₃H₅)(phosphoramidite)] complex (0.030 mmol, 1.0 equiv) in CD₂Cl₂ (1 mL) is transferred via cannula into a Schlenk tube containing solid AgSbF₆ (0.030 mmol, 1.0 equiv). A white precipitate of AgCl forms immediately. The suspension is stirred for ca. 2 h, then the solution is filtered through Celite directly into a NMR tube equipped with a J. Young-type valve.

In some cases the product was isolated by evaporating the solvent and washing the resulting solid with Et₂O. The elemental analyses for these complexes are poor, since they are coordinatively unsaturated and tend to absorb water.

[Pd(C₄H₇)(S,S,S-1)]SbF₆, 15: yellowish-white solid, yield 75%. MALDI MS: 1184 (M⁺ − C₃H₅ + L), 686 (M⁺), 646 (M⁺ − C₃H₅), 540 (M⁺ − C₃H₅ − Pd).

[Pd(C₃H₅)(2)]SbF₆, 19: yellowish-white solid, yield 65%. MALDI MS: 600 (M⁺), 546 (M⁺ − CH₂CCH₃CH₂), 438 (M⁺ − CH₂CCH₃CH₂ − Pd).

[Pd(C₃H₅)(3)]SbF₆, 21: yellowish-white solid, yield 70%. MALDI MS: 927 (M⁺ − C₃H₅ + L), 556 (M⁺), 518 (M⁺ − C₃H₅), 410 (M⁺ − C₃H₅ − Pd).

Synthesis of [PtCl(allyl)(phosphoramidite)]. A solution of the P-donor ligand (0.180 mmol, 2.00 equiv) in CH₂Cl₂ (10 mL) is slowly added, under stirring, to a suspension of the dinuclear species

[Pd(μ-Cl)(C₃H₅)]₂ (0.090 mmol, 1.05 equiv) in CH₂Cl₂ (10 mL). After the addition is finished, particles of platinum dimer are still visible in suspension. The mixture is stirred until it clears up (about 30 min), then it is filtered to remove the excess platinum precursor. The solvent is removed under reduced pressure, giving a solid, which is washed with diethyl ether and dried under vacuum.

[PtCl(C₃H₅)(S,R,R-1)], 12: yellowish-white solid, yield 73%. Anal. Calcd for C₃₉H₃₅ClNO₂PPt · CD₂Cl₂: C, 53.63; H, 4.13; N, 1.56. Found: C, 53.35; H, 3.82; N, 1.33. MALDI MS: 1317 (M⁺ − Cl + 1), 875 (M⁺ − Cl − C₃H₅ + HPA).

[PtCl(C₃H₅)(2)], 13: whitish solid, yield 85%. Anal. Calcd for C₃₁H₃₁ClNO₂PPt: C, 52.36; H, 4.39; N, 1.97. Found: C, 52.03; H, 4.32; N, 1.95. MALDI MS: 1114 (M⁺ − Cl + 2), 675 (M⁺ − Cl), 668 (M⁺ − C₃H₅), 633 (M⁺ − Cl − C₃H₅).

[PtCl(C₃H₅)(3)], 14: whitish solid, yield 80%. MALDI MS: 645 (M⁺ − Cl), 603 (M⁺ − Cl − C₃H₅). Although from the ³¹P NMR spectrum only the desired product can be detected, the elemental analysis data are poor.

Synthesis of [Pt(allyl)(phosphoramidite)]SbF₆ (NMR sample). A solution of the suitable [PtCl(C₃H₅)(phosphoramidite)] complex (0.030 mmol, 1.0 equiv) in CD₂Cl₂ (1 mL) is transferred via cannula into a Schlenk tube containing solid AgSbF₆ (0.030 mmol, 1.0 equiv). A white precipitate of AgCl forms immediately. The suspension is then stirred for 10 min, and the solution is filtered through Celite directly into a NMR tube equipped with a J. Young-type valve.

DFT Calculations. Density functional theory (DFT) calculations[31] were carried out with the Amsterdam Density Functional (ADF2006) program.[32] Gradient-corrected geometry optimizations[33] without symmetry constraints were performed using the local density approximation of the correlation energy (Vosko, Wilk, Nusair)[34] and the exchange−correlations functionals of Perdew−Wang (PW91).[35] Relativistic effects were taken into account with the ZORA approximation.[36] A triple-ζ Slater-type orbital (STO) basis set augmented by two polarization functions was used for Pd, Ru, P, O, C, N, and H. A frozen core approximation was used to treat the core electrons: (1s) for C, O, and N, (1s, 2p) for P, ([1−3]s, [2−3]p, 3d) for Pd and Ru. Mayer indices[37] were used as bond strength indicators.

The energy decomposition analysis (EDA) developed by Ziegler and Rauk[38] was applied to the PW91-optimized geometries to analyze the interactions between the metals and the C−C bonds. The bond dissociation energy (Δ$E = −D_e$) between two fragments is taken as the sum of two contributions, Δ$E = ΔE_{prep} + ΔE_{int}$, where ΔE_{prep} is the energy required to reorganize the fragments from their equilibrium geometry to the geometry of the complex; ΔE_{int} is the interaction energy between the two fragments in the complex and can be divided into three components: Δ$E_{elec} + ΔE_{pauli} + ΔE_{orb}$.

(31) Parr, R. G., Yang, W., *Density-Functional Theory of Atoms and Molecules*; Clarendon Press: New York, 1989.

(32) (a) *ADF 2004. 01, SCM, Theoretical Chemistry*; Vrije Universiteit: Amsterdam, The Netherlands, http://www.scm.com. (b) Te Velde, G.; Bickelhaupt, F. M.; Baerends, E. J.; Fonseca Guerra, C.; Van Gisbergen, S. J. A.; Snijders, J. G.; Ziegler, T. *J. Comput. Chem.* **2001**, *22* (9), 931–967. (c) Guerra, C. F.; Snijders, J. G.; Te Velde, G.; Baerends, E. J. *Theor. Chem. Acc.* **1998**, *99* (6), 391–403.

(33) (a) Versluis, L.; Ziegler, T. *J. Chem. Phys.* **1988**, *88* (1), 322–328. (b) Fan, L.; Ziegler, T. *J. Chem. Phys.* **1991**, *95* (10), 7401–7408.

(34) Vosko, S. H.; Wilk, L.; Nusair, M. *Can. J. Phys.* **1980**, *58* (8), 1200–1211.

(35) Perdew, J. P.; Chevary, J. A.; Vosko, S. H.; Jackson, K. A.; Pederson, M. R.; Singh, D. J.; Fiolhais, C. *Phys. Rev. B: Condens. Matter Mater. Phys.* **1992**, *46* (11), 6671–6687.

(36) van Lenthe, E.; Ehlers, A.; Baerends, E.-J. *J. Chem. Phys.* **1999**, *110* (18), 8943–8953.

(37) (a) Mayer, I. *Chem. Phys. Lett.* **1983**, *97* (3), 270–274. (b) Mayer, I. *Int. J. Quantum Chem.* **1984**, *26* (1), 151–154.

(38) (a) Ziegler, T.; Rauk, A. *Theor. Chim. Acta* **1977**, *46* (1), 1–10. (b) Ziegler, T.; Rauk, A. *Inorg. Chem.* **1979**, *18* (6), 1558–1565.

The ΔE_{elec} term corresponds to the electrostatic interaction energy between the fragments; ΔE_{pauli} is the repulsive interaction between the fragments as a result of the fact that two electrons with the same spin are unable to occupy the same region in space; ΔE_{orb} is associated with the orbital interaction energy (covalent bond formation).

Single-point DFT/B3LYP[39] calculations using the previously optimized geometries (ADF/PW91) were also performed with Gaussian03[40] using the standard LanL2DZ basis set with the associated ECP[41] for Ru and Pd, and a standard 6-311G** basis set for the remaining elements. Wiberg Indices[42] were obtained from a natural population (NPA) analysis[43] and were also used as bond strength indicators. NMR chemical shifts were calculated using the Gaussian03 implementation of the gauge-independent atomic orbital (GIAO) method.[44]

Supporting Information Available: Distances, Mayer indices and Wiberg indices for the two Pd complexes **17** and **17*** are given in Table S1, and for the two Ru complexes Ru and Ru* in Table S2. Table S3 gives DFT calculated ^{13}C relative* chemical shifts for complexes **17**, **17***, Ru, and Ru*. This material is available free of charge via the Internet at http://pubs.acs.org.

OM8000636

(39) Lee, C.; Yang, W.; Parr, R. G. *Phys. Rev. B: Condens. Matter Mater. Phys.* **1988**, *37* (2), 785–789.

(40) , Frisch, M. J.; Trucks, G. W.; Schlegel, H. B.; Scuseria, G. E.; Robb, M. A.; Cheeseman, J. R.; Zakrzewski, V. G.; Montgomery, J. A., Jr.; Stratmann, R. E.; Burant, J. C.; Dapprich S.; Millam, J. M.; Daniels, A. D.; Kudin, K. N.; Strain, M. C.; Farkas, O.; Tomasi, J.; Barone, V.; Cossi, M.; Cammi, R.; Mennucci, B.; Pomelli, C.; Adamo, C.; Clifford, S.; Ochterski, J.; Petersson, G. A.; Ayala, P. Y.; Cui, Q.; Morokuma, K.; Rega, N.; Salvador. Dannenberg, J. J.; Malick, D. K.; Rabuck, A. D.; Raghavachari, K.; Foresman, J. B.; Cioslowski, J.; Ortiz, J. V. Baboul, A. G.; Stefanov, B. B.; Liu, G.; Liashenko, A.; Piskorz, P.; Komaromi, I.; Gomperts, R. L.Martin, R.; Fox, D. J.; Keith, T.; Al-Laham, A.; Peng, C. Y.; Nanayakkara, A. Challacombe, M.; Gill, P. M. W.; Johnson, B.; Chen, W.; Wong, M. W.; Andres, J. L.; Gonzalez, C.; Head-Gordon, M.; Replogle, E. S.; Pople, J. A. *Gaussian 03*; Gaussian, Inc.: Wallingford, CT, 2004.

(41) (a) Dunning, T. H. J., Hay, P. J. In *Modern Theoretical Chemistry*l Schaefer, H. F. I., Ed.; Plenum: New York, 1976; Vol. 3, p 1. (b) Wadt, W. R.; Hay, P. J. *J. Chem. Phys.* **1985**, *82* (1), 284–298. (c) Hay, P. J.; Wadt, W. R. *J. Chem. Phys.* **1985**, *82* (1), 270–283. (d) Hay, P. J.; Wadt, W. R. *J. Chem. Phys.* **1985**, *82* (1), 299–310.

(42) Wiberg, K. B. *Tetrahedron* **1968**, *24* (3), 1083–1096.

(43) (a) Carpenter, J. E. Ph.D. Thesis, University of Wisconsin, Madison, WI, 1987. (b) Foster, J. P.; Weinhold, F. *J. Am. Chem. Soc.* **1980**, *102* (24), 7211–7218. (c) Reed, A. E.; Weinhold, F. *J. Chem. Phys.* **1983**, *78* (6), 4066–4073. (d) Reed, A. E.; Weinhold, F. *J. Chem. Phys.* **1985**, *83* (4), 1736–1740. (e) Reed, A. E.; Weinstock, R. B.; Weinhold, F. *J. Chem. Phys.* **1985**, *83* (2), 735–746. (f) Reed, A. E.; Curtiss, L. A.; Weinhold, F. *Chem. Rev.* **1988**, *88* (6), 899–926. (g) Weinhold, F., Carpenter, J. E. *The Structure of Small Molecules and Ions*; Plenum Press: New York, 1988.

(44) (a) Ditchfield, R. *Mol. Phys.* **1974**, *27* (4), 789–807. (b) Dodds, J. L.; McWeeny, R.; Sadlej, A. J. *Mol. Phys.* **1977**, *34* (6), 1779–1791. (c) Wolinski, K.; Hinton, J. F.; Pulay, P. *J. Am. Chem. Soc.* **1990**, *112* (23), 8251–8260.